Research Square

Preprints are preliminary reports that have not undergone peer review.
They should not be considered conclusive, used to inform clinical practice,
or referenced by the media as validated information.

Integrated Groundwater Quality Assessment using Hydrogeochemical Characterization and Water Quality Index: A Case Study of Osun State University Campus, Southwestern Nigeria

Solomon M. Jekayinfa[1]

solomon.jekayinfa@uniosun.edu.ng

Osun State University

Rasaq A. Azeez[1]

Osun State University

Olabanji A. Ojo[1]

Osun State University

Research Article

Keywords: Hydrogeochemistry, Water Quality Index, Piper diagram, Gibbs diagram, Groundwater quality, Basement complex, Nigeria

Posted Date: October 23rd, 2026

DOI: https://doi.org/10.21203/rs.3.rs-11205655/v1

License: This work is licensed under a Creative Commons Attribution 4.0 International License. Read Full License

Additional Declarations: No competing interests reported.

Abstract

Groundwater quality assessment in crystalline basement terrains presents unique challenges due to the heterogeneous nature of aquifers and vulnerability to both geogenic and anthropogenic contamination. This study presents a comprehensive hydrogeochemical assessment of groundwater from ten boreholes within the Osun State University campus, Osogbo, Southwestern Nigeria, as a case study of institutional water supply in a crystalline basement terrain. Groundwater samples were analysed for physicochemical parameters, major ions, trace metals, toxic heavy metals, and microbiological indicators. Hydrogeochemical characterisation employed Piper trilinear diagrams, Gibbs diagrams, and ion ratio analysis to elucidate dominant geochemical processes. The Water Quality Index (WQI) was computed using the weighted arithmetic method to assess overall suitability for drinking purposes. Results revealed slightly acidic to neutral groundwater (pH 6.3–7.1) with uniform Calcium-Magnesium-Bicarbonate (Ca–Mg–HCO_3) hydrogeochemical facies in all samples, indicating silicate weathering as the dominant geochemical process. Gibbs diagram analysis confirmed rock-water interaction as the primary control on groundwater chemistry. Ion ratios (Na^+/Cl^-, Ca^{2+}/Mg^{2+}, Cl^-/HCO_3^-) corroborated silicate weathering and meteoric recharge with minimal evaporative concentration. Toxic heavy metals (As, Cd, Pb, Hg) were below detection limits, indicating minimal anthropogenic pollution. However, iron concentrations exceeded WHO guidelines in 90% of samples (up to 1.00 mg/L), and turbidity exceeded permissible limits in 100% of samples (up to 52 NTU). Microbiological analysis revealed total coliform contamination in all samples (> 180 MPN/100mL), representing the most immediate health risk and rendering the groundwater unfit for direct consumption. One borehole (BH7, Multidisciplinary Research Laboratory) exhibited elevated EC (2,340 µS/cm) and TDS (1,521 mg/L), indicating localized contamination from laboratory activities. WQI values ranged from 58.94 to 209.00, classifying 40% of samples as 'Good,' 50% as 'Poor,' and 10% as 'Very Poor.' The study underscores the necessity of routine monitoring, disinfection, and iron removal interventions for sustainable groundwater resource management in basement complex terrains.

1. INTRODUCTION

Groundwater constitutes the most reliable freshwater source in tropical crystalline basement terrains, particularly in developing countries where surface water resources are increasingly compromised by seasonal variability and anthropogenic pollution (Todd & Mays, 2005; MacDonald et al., 2012; Adeyeye et al., 2025). Crystalline basement terrains cover approximately 50% of Nigeria's landmass and present unique hydrogeological challenges due to their negligible primary porosity, restricting groundwater occurrence to secondary porosity features such as weathered zones, fractures, joints, and faults (Rahaman, 1988; Wright, 1992). In Nigeria, over 60% of the population depends on groundwater for domestic, agricultural, and industrial needs, with basement complex aquifers serving as primary sources across southwestern regions (Olorunfemi & Fasuyi, 1993; Adelana et al., 2008).

The hydrogeochemical composition of groundwater in basement complex aquifers reflects its interaction with the geological environment and anthropogenic influences. It reveals the processes that control groundwater evolution, such as dissolution, ion exchange, precipitation, and oxidation-reduction reactions (Appelo & Postma, 2005; Raju et al., 2024). Parameters such as pH, electrical conductivity (EC), total dissolved solids (TDS), and major ion concentrations provide valuable insights into aquifer processes and the suitability of water for various uses (Hem, 1985; Adesiyan et al., 2018; Taiwo et al., 2020). Hydrogeochemical analysis elucidates the evolution of groundwater chemistry through rock-water interactions, revealing mineralization processes, contamination

sources, and overall water suitability (Gibbs, 1970; Freeze & Cherry, 1979; Appelo & Postma, 2005; Sahu et al., 2024).

Recent studies have demonstrated the utility of integrated approaches combining hydrogeochemical characterization with water quality indices and multivariate statistical techniques for comprehensive groundwater assessment (Gani et al., 2024; Hossain et al., 2024; Masitoh et al., 2025). These approaches enable the identification of dominant geochemical processes, quantification of contamination levels, and assessment of overall water suitability for various uses (Boukich et al., 2025; Xu et al., 2025).

This study aims to characterize the hydrogeochemical facies of groundwater within the UNIOSUN campus, identify the dominant geochemical processes controlling groundwater chemistry, assess the spatial distribution of physicochemical parameters, trace metals, and microbiological contamination, and compute the Water Quality Index (WQI) for groundwater suitability assessment. As a campus-scale case study, this work demonstrates an integrated assessment framework that can be replicated at other institutional and community water supply sites within basement complex terrains, while acknowledging that the specific findings are limited to the study area.

1.1 Research Objectives

The specific objectives of this study are:

1. To characterize the hydrogeochemical facies of groundwater within the UNIOSUN campus using Piper trilinear diagrams
2. To identify the dominant geochemical processes controlling groundwater chemistry using Gibbs diagrams and ion ratio analysis
3. To assess the spatial distribution of physicochemical parameters, trace metals, and microbiological contamination
4. To compute and classify the Water Quality Index (WQI) for groundwater suitability assessment
5. To evaluate the implications of groundwater quality for sustainable water resource management in basement complex terrains

This study addresses the following scientific questions: (i) What are the dominant hydrogeochemical processes controlling groundwater chemistry in the study area? (ii) How does groundwater quality vary spatially across the campus? (iii) What are the primary contaminants of concern and their potential sources? (iv) What management interventions are required to ensure safe water supply?

2. STUDY AREA

2.1 Location and Accessibility

The study area is within the main campus of Osun State University (UNIOSUN), Southwestern Nigeria (Fig. 1). It lies between latitudes 7°45'N and 7°50'N and longitudes 4°30'E and 4°37'E, covering approximately 2 km². The area is accessible via the Osogbo–Ibadan and Osogbo–Ede highways, with internal road networks connecting academic, administrative, and residential zones

2.2 Climate and Vegetation

The climate is humid tropical, characterized by distinct wet (April–October) and dry (November–March) seasons. Mean annual rainfall ranges from 1,200 to1,400 mm, with a double maximum in July and September (NIMET, 2023), characteristic of the tropical savanna climate typical of Southwestern Nigeria (Olorunfemi & Fasuyi, 1993). Temperatures average 27°C (range: 25–32°C), while relative humidity varies between 60% and 85% (NIMET, 2023). The natural vegetation is derived savanna, comprising grasses interspersed with trees including *Terminalia* spp., *Albizia zygia*, and *Daniellia oliveri*, though urbanization has significantly modified native vegetation patterns (Adeyemo et al., 2023).

2.3 Geological Setting

Osogbo lies within the Precambrian Basement Complex of Southwestern Nigeria, part of the Pan-African mobile belt (Rahaman, 1988; Olorunfemi & Ojo, 2003). The dominant lithological unit around the UNIOSUN campus is amphibolite schist (Fig. 2), which forms part of the Precambrian Basement Complex of Southwestern Nigeria. This schistose rock is characterised by its foliated texture, composed primarily of amphibole minerals (such as hornblende) with plagioclase feldspar, and occasionally intercalated with quartz-rich bands. The weathered products of this amphibolite schist give rise to the clayey to sandy-clay overburden observed across the campus, influencing both the hydrogeochemical characteristics and the groundwater potential of the area (Bayowa et al., 2023).

2.4 Hydrogeological Setting

The hydrogeological regime consists of two distinct aquifer systems: a shallow unconfined aquifer within the weathered regolith (saprolite), typically 5–25 m thick, and a deeper semi-confined aquifer within fractured bedrock, occurring at a depth range of 30–60 m (Oyeyemi et al., 2019; Olawuyi & Katchy, 2016). The weathered layer, comprising clayey sand to sandy clay, provides storage capacity, while fracture networks facilitate groundwater flow and good borehole yield (Olorunfemi & Ojo, 2003; Olorunfemi & Fasuyi, 1993).

Groundwater flow in the study area follows the general topographic gradient, with recharge occurring primarily through direct rainfall infiltration in elevated areas and discharge toward lower topographic positions and stream valleys. Recharge rates are estimated at 5–15% of annual precipitation (Adelana et al., 2008). The weathered regolith aquifer typically exhibits transmissivity values ranging from 1 to 50 m²/day, while the fractured bedrock aquifer may achieve transmissivity values of 10–100 m²/day where fracture connectivity is well-developed (Olorunfemi & Fasuyi, 1993). Borehole yields in the area range from 0.5 to 5.0 L/s, with higher yields associated with zones of enhanced fracturing and thicker weathered profiles.

Current groundwater exploitation within the campus is primarily through ten production boreholes equipped with submersible pumps, supplying water for domestic, institutional, and research purposes. Static water levels measured during this study ranged from 5.7 to 6.5 m below ground level, indicating relatively shallow water tables that facilitate contaminant migration from surface sources.

2.5 Aquifer System Investigated

This study focuses on the shallow unconfined aquifer system within the weathered regolith (saprolite). All sampled boreholes are completed within the weathered overburden at depths ranging from 25 to 45 m, with screen intervals positioned within the saprolite zone. The weathered regolith aquifer was selected for investigation because: (i) it represents the primary source of groundwater supply for the campus; (ii) it is most

vulnerable to surface contamination due to its shallow depth and unconfined nature; and (iii) previous studies have identified water quality variability within this aquifer system (Oyeyemi et al., 2019). The deeper fractured bedrock aquifer was not sampled in this study due to limited accessibility and the focus on assessing the shallow groundwater resources currently being exploited.

3. MATERIALS AND METHODS

3.1 Sampling Strategy

A purposive sampling strategy was employed to select ten groundwater sampling locations representing spatial variability in land use across the campus, all underlain by the same amphibolite schist lithology (Fig. 1). Sampling points included the Administrative Building (BH1), SET Building (BH2), Multipurpose Store (BH3), Engineering Building (BH4), Multipurpose Complex (BH5), Anatomy Complex (BH6), Multidisciplinary Research Laboratory (BH7), Staff Office (BH8), Auditorium Hall (BH9), and Water Factory (BH10).

Groundwater sampling was conducted in November 2024, during the transition from the wet season to the dry season, representing baseline conditions for groundwater quality assessment. Boreholes were purged for 10–15 minutes to remove stagnant water before sample collection, following standard procedures for groundwater quality investigations (ASTM D6452, 2005). This purging step is essential to ensure that collected samples accurately represent ambient groundwater chemistry rather than water that has remained stagnant within the borehole casing (ASTM D6452, 2005; Cherry et al., 2020).

3.2 Field Measurements

Field measurements of pH, temperature, electrical conductivity (EC), and total dissolved solids (TDS) were conducted in-situ using calibrated portable meters (Hanna Instruments HI98129), following standard protocols for field parameter measurement (USGS, 2006; APHA, 2023). The meter was calibrated daily using standard buffer solutions (pH 4.0, 7.0, and 10.0) and conductivity standards (1413 µS/cm). Static water levels were measured using a Geotech dipmeter.

Groundwater samples were collected in pre-cleaned 1-litre polyethylene bottles, with samples for cation analysis acidified to pH < 2 using ultrapure nitric acid to prevent metal precipitation and adsorption onto container walls (APHA, 2023; ASTM D6517-18, 2023). Samples were transported under chilled conditions to the laboratory and stored at 4°C until analysis.

3.3 Laboratory Analysis

Major Anions: Major anions (Cl^-, SO_4^{2-}, NO_3^-, NO_2^-) were determined by ion chromatography using a Dionex ICS-1100 system, following established methods for anion analysis in groundwater (Standard Methods, 2023; ISO 10304-1, 2007). Bicarbonate (HCO_3^-) was analysed by the titrimetric method using 0.1N HCl, a standard technique for alkalinity determination in water samples (APHA, 2023; Rice et al., 2012).

Major Cations: Major cations (Ca^{2+}, Mg^{2+}, Na^+, K^+) were analysed using Atomic Absorption Spectrophotometry (AAS) following standard protocols (APHA, 2023).

Trace and Heavy Metals: Trace metals (Fe, Cu, Zn, Cr, Al) were analysed by flame atomic absorption spectrophotometry (AAS), while toxic heavy metals (As, Cd, Pb, Hg) were analysed using graphite furnace atomic

absorption spectrophotometry (GF-AAS) with detection limits of 0.001 mg/L (Townsend et al., 2001; Marin et al., 2010; US EPA Method 200.9).

Microbiological Analysis: Microbiological analysis for total coliform was conducted using the multiple-tube fermentation technique (most probable number method), following standard methods for the bacteriological examination of water (APHA, 2023; Rice et al., 2012). The procedure involved three stages:

(i) Presumptive test: Sample volumes of 50 mL, 10 mL, and 1 mL were inoculated into triplicate tubes containing lauryl tryptose broth with Durham tubes. The tubes were incubated at 37°C for 24–48 hours. Gas production within the Durham tubes constituted a presumptive positive result for coliform bacteria.

(ii) Confirmed test: Presumptive positive tubes were streaked onto MacConkey agar and Eosin Methylene Blue (EMB) agar and incubated at 37°C for 24 hours. Growth on MacConkey agar with characteristic pink colonies confirmed total coliforms. Growth on EMB agar with a metallic green sheen confirmed E. coli.

(iii) Completed test: Presumptive positive results from Salmonella-Shigella agar were recorded for enteric pathogen screening; however, confirmatory biochemical testing (e.g., triple sugar iron, citrate, urease) was not performed, and these results are therefore reported as presumptive only.

Results were expressed as most probable number (MPN) per 100 mL of water sample, calculated using standard MPN tables (APHA, 2023). The detection limit of the method was <1.8 MPN/100 mL for the 50 mL, 10 mL, and 1 mL dilution series. Replicate analyses were performed in triplicate for each sample volume.

Quality Assurance: Quality assurance included analysis of blanks, duplicate samples, and certified reference materials. Analytical precision was within ±5% for major ions and ±10% for trace metals. Charge balance errors were calculated for all samples to validate analytical accuracy, and only samples with charge balance errors within ±10% were considered acceptable for hydrogeochemical interpretation (Freeze & Cherry, 1979). Instrument calibration was performed daily using certified standard solutions, and reagent blanks were analysed with each batch of samples to monitor potential contamination.

3.4 Water Quality Index

The Water Quality Index (WQI) was computed using the weighted arithmetic index method (Brown et al., 1972). Nine parameters were selected based on their significance for drinking water quality: pH, EC, TDS, turbidity, total hardness, Cl^-, NO_3^-, Fe, and total coliforms (Table S1). Total coliform was included to ensure that the WQI reflects microbiological quality, which is critical for assessing the overall suitability of groundwater for drinking purposes.

Each parameter was assigned a weight (w_i) ranging from 2 (least significant) to 5 (most significant) based on its relative importance to human health (Table S1, Supplementary Materials). The relative weight (W_i) was calculated using Equation 1:

Equation 1: $W_i = w_i / \Sigma(w_i)$

where $\Sigma(w_i)$ is the sum of all parameter weights. The quality rating scale (Q_i) for each parameter was computed using Equation 2:

Equation 2: $Q_i = (C_i / S_i) \times 100$

where C_i is the concentration of each parameter in each water sample, and S_i is the WHO (2022) drinking water guideline value for the respective parameter. The WQI was then calculated using Equation 3:

Equation 3: $WQI = \Sigma(W_i \times Q_i)$

Water quality was classified according to the following scheme: <50 = Excellent; 51–100 = Good; 101–200 = Poor; 201–300 = Very Poor; >300 = Unsuitable for drinking.

3.5 Hydrogeochemical Data Analysis

We used hydrogeochemical data to generate Piper trilinear diagrams for facies classification and Gibbs diagrams to identify dominant geochemical processes (Xu et al., 2025; Boukich et al., 2025; Masitoh et al., 2025). The Piper diagram enables the visualization of hydrogeochemical facies evolution and the classification of water types based on major ion chemistry, while the Gibbs diagram facilitates the distinction between rock-dominated, evaporation-dominated, and precipitation-dominated controls on water chemistry (Xu et al., 2025; Xiangxiang et al., 2025; Masitoh et al., 2025).

Ion ratios (Na^+/Cl^-, Ca^{2+}/Mg^{2+}, Cl^-/HCO_3^-) were calculated using milliequivalents per litre (meq/L) to elucidate geochemical evolution, as these ratios provide critical insights into the dominant processes governing groundwater chemistry, including silicate weathering, cation exchange, and mineral dissolution (Avenbuan et al., 2025; Masitoh et al., 2025). The Na^+/Cl^- ratio helps distinguish between halite dissolution and silicate weathering sources of sodium, while the Ca^{2+}/Mg^{2+} ratio aids in identifying the specific carbonate minerals involved in water-rock interactions (Avenbuan et al., 2025).

3.6 Statistical Analysis

Descriptive statistics (mean, median, standard deviation, range) were computed for all Hydrogeochemical parameters. Pearson correlation analysis was performed to examine relationships among Hydrogeochemical parameters and identify potential controlling factors. All statistical analyses were conducted using SPSS version 26.0 and Microsoft Excel 2019.

3.7 Limitations of the Study

The authors acknowledge the following limitations: (i) the study is based on ten boreholes within a single campus, which may limit the generalizability of findings to broader basement complex terrains; (ii) sampling was conducted during a single campaign, and seasonal variations in groundwater quality were not captured; (iii) the deeper fractured bedrock aquifer was not sampled, and conclusions are restricted to the shallow weathered regolith aquifer; (iv) the BH7 sample exhibited anomalous EC and TDS values that may reflect localized contamination rather than ambient groundwater quality, and this sample is discussed separately; and (v) spatial interpolation of WQI values assumes continuous variation between sampling points, which may not fully capture local-scale heterogeneity. These limitations should be considered when interpreting the study findings.

4. RESULTS

4.1 Hydrogeochemical Characteristics

4.1.1 Physicochemical Parameters

The physicochemical characteristics of groundwater samples are summarised in Table 1. pH values ranged from 6.3 to 7.1, indicating slightly acidic to neutral conditions. Five samples (50%) fell below the WHO (2022) lower permissible limit of 6.5, with the lowest pH (6.3) recorded at BH8 (Staff Office) and BH9 (Auditorium Hall). The slightly acidic nature reflects carbonic acid from dissolved CO_2 and organic matter decomposition in the soil zone (Freeze & Cherry, 1979; Hem, 1985; Appelo & Postma, 2005). In shallow groundwater systems, the infiltration of meteoric water through the unsaturated zone facilitates the dissolution of biogenic carbon dioxide produced by root respiration and microbial decomposition of organic matter, leading to the formation of carbonic acid (H_2CO_3), which subsequently lowers the pH of the groundwater (Drever, 1997; Langmuir, 1997). This phenomenon is widely documented in basement complex terrains where thin overburden and rapid recharge promote active soil-water-rock interactions (Olorunfemi & Fasuyi, 1993; Adelana et al., 2008; Taiwo et al., 2020).

Table 1: Physicochemical Parameters of Groundwater Samples

S/N	LOCATION NAME	SAMPLE CODE	pH	TEMPERATURE (°C)	Turbidity (NTU)	Electrical Conductivity (EC) (mg/L)	TDS (mg/L)
	WHO (2022) Standard		**6.5-8.5**	**-**	**5**	**-**	**1000**
1	ADMIN BUILDING	BH 1	6.9	28.7	08.00	245.1	156.9
2	SET BUILDING	BH 2	6.4	28.6	52.00	263.5	168.6
3	MULTIPURPOSE STORE	BH 3	6.4	28.6	48.00	380.7	243.6
4	ENGINEERING BUILDING	BH 4	6.4	28.4	44.00	263.2	168.4
5	MULTIPURPOSE COMPLEX	BH 5	6.5	28.3	08.00	250.1	160.1
6	ANATOMY COMPLEX	BH 6	6.9	28.4	48.00	579.2	370.7
7	MULTIDISCIPLINARY RESEARCH LABORATORY	BH 7	7.1	28.60	52.00	2,340.0	1,521.0
8	STAFF OFFICE	BH 8	6.3	25.70	10.00	223.20	142.8
9	AUDITORIUM HALL	BH 9	6.3	28.6	44.00	133.80	85.6
10	WATER FACTORY	BH 10	6.9	28.60	10.00	372.10	238.1

Temperature values ranged from 25.7°C to 28.7°C (mean: 28.2°C), consistent with tropical groundwater systems. Turbidity exhibited considerable variation (8.00–52.00 NTU), with all ten samples exceeding the WHO (2022) guideline of 5 NTU. The highest turbidity values (52 NTU) occurred at BH2 (SET Building) and BH7 (Multidisciplinary Research Laboratory), while BH1 (Admin Building) and BH5 (Multipurpose Complex) recorded the lowest (8 NTU).

Elevated turbidity in groundwater from basement complex terrains is primarily attributable to the presence of suspended colloidal particles, including fine-grained clay minerals (kaolinite, illite), silt-sized quartz grains, and precipitated iron oxides/hydroxides (Hem, 1985; Appelo & Postma, 2005). In weathered crystalline basement aquifers, the physical disintegration of feldspars and ferromagnesian minerals produces fine particulates that remain suspended in the groundwater column, particularly during pumping or when flow velocities are sufficient to entrain these particles (Freeze & Cherry, 1979; Olobaniyi & Owoyemi, 2006). Additionally, the oxidation of dissolved ferrous iron (Fe^{2+}) to ferric iron (Fe^{3+}) upon exposure to atmospheric oxygen leads to the formation of reddish-brown colloidal iron hydroxide precipitates ($Fe(OH)_3$), which significantly contribute to turbidity, especially in boreholes with high iron concentrations (Hem, 1985; Ehirim & Nwankwo, 2015). The elevated turbidity observed at BH2 and BH7, which also recorded high iron concentrations (1.00 mg/L and 0.80 mg/L, respectively), suggests that iron oxidation is a significant contributor to turbidity at these locations.

Electrical conductivity (EC) ranged from 133.8 to 2,340.0 µS/cm, exhibiting significant spatial variability. Excluding the anomalous BH7 value (2,340.0 µS/cm), EC ranged from 133.8–579.2 µS/cm (mean: 301.2 µS/cm). The BH7 anomaly, approximately 4.5 times higher than the second-highest value (BH6: 579.2 µS/cm), suggests localized contamination, possibly from laboratory activities given its location at the Multidisciplinary Research Laboratory. This sample is discussed separately in Section 4.1.4. For the remaining samples, EC values indicate moderate mineralization typical of basement complex aquifers."

"TDS ranged from 85.6 to 1,521.0 mg/L (mean: 325.6 mg/L). Excluding BH7, TDS ranged from 85.6–370.7 mg/L (mean: 192.8 mg/L), well below the WHO guideline of 1,000 mg/L. The BH7 value (1,521 mg/L) exceeds the WHO aesthetic guideline and is consistent with the elevated EC at this location.

4.1.2 Major Ions and Hydrogeochemical Facies

Major ion concentrations are presented in Table 2. Calcium (Ca^{2+}) ranged from 3.2–168.0 mg/L (mean: 35.4 mg/L), with an anomalously high value at BH3 (168 mg/L) indicating a localized calcium source. Excluding this outlier, Ca^{2+} ranged from 3.2–52.8 mg/L, typical for basement terrains. Magnesium (Mg^{2+}) ranged from 0.50–22.0 mg/L (mean: 4.97 mg/L), with the highest concentration at BH7 (22.0 mg/L). Sodium (Na^{+}) ranged from 0.20–2.70 mg/L (mean: 2.04 mg/L), while potassium (K^{+}) was consistently low (0.00–2.50 mg/L; mean: 1.87 mg/L).

Table 2: Major ion concentrations in groundwater samples (mg/L)

Sample Code	Ca^{2+}	Mg^{2+}	Na^{+}	K^{+}	HCO_3^{-}	Cl^{-}	SO_4^{2-}	NO_3^{-}	Hardness
BH 1	15.2	0.50	1.00	0.8	78.0	16.0	9.00	0.240	40.0
BH 2	12.8	1.50	2.50	2.30	128.0	7.5	25.00	0.050	38.0
BH 3	16.8	4.50	2.30	2.10	206.0	6.5	21.00	0.001	60.0
BH 4	8.0	4.50	2.40	2.20	120.0	9.5	22.00	0.030	38.0
BH 5	4.8	4.50	0.20	0.00	78.0	15.5	0.00	0.064	30.0
BH 6	46.1	0.70	2.40	2.20	416.0	9.5	20.00	0.001	118.0
BH 7	52.8	22.00	2.50	2.30	204.0	11.5	25.00	0.018	220.0
BH 8	4.0	5.50	2.00	1.80	46.0	11.0	12.00	0.049	32.0
BH 9	3.2	5.00	2.70	2.50	28.0	11.5	24.00	0.013	28.0
BH 10	19.2	3.00	2.30	2.10	100.0	11.0	21.00	0.014	60.0
WHO (2022)	**-**	**-**	**200**	**-**	**-**	**250**	**250**	**50**	**500**
Note: (-) indicates no guideline value specified									

Bicarbonate (HCO_3^{-}) dominated the anion suite, ranging from 28.0–416.0 mg/L (mean: 148.4 mg/L), with the highest value at BH6 (416 mg/L). Chloride (Cl^{-}) ranged from 6.5–16.0 mg/L (mean: 10.95 mg/L), well below the WHO guideline of 250 mg/L. Sulphate (SO_4^{2-}) ranged from 0.00–25.00 mg/L (mean: 17.9 mg/L), with all samples below the WHO guideline of 250 mg/L.

Nitrate (NO_3^{-}) concentrations were remarkably low (0.001–0.240 mg/L; mean: 0.048 mg/L), orders of magnitude below the WHO guideline of 50 mg/L, indicating minimal agricultural or sewage impacts.

Total hardness ranged from 28.0–220.0 mg/L (mean: 66.4 mg/L), classifying groundwater as soft to moderately hard according to the standard classification scheme (Sawyer & McCarty, 1967; WHO, 2022), with only BH7 exhibiting hard water characteristics (>200 mg/L).

The Piper trilinear diagram (Fig. 3) reveals that all ten groundwater samples plot within the Calcium-Magnesium-Bicarbonate ($Ca–Mg–HCO_3$) field. This indicates that silicate weathering is the dominant geochemical process controlling groundwater chemistry in the study area. No distinct Sodium-Bicarbonate ($Na–HCO_3$) facies was observed. The predominance of $Ca–Mg–HCO_3$ water type in 100% of the samples (10 out of 10) indicates that groundwater chemistry is primarily controlled by the dissolution of silicate minerals present in the underlying amphibolite schist bedrock (Rahaman, 1988; Bayowa et al., 2023). The weathering of plagioclase feldspar (anorthite component) and ferromagnesian minerals (hornblende, biotite) releases Ca^{2+}, Mg^{2+}, and HCO_3^{-} into solution through reactions with carbonic acid derived from atmospheric CO_2 and soil zone organic matter decomposition (Drever, 1997; Langmuir, 1997).

The dominance of the Ca–Mg–HCO_3 hydrogeochemical facies indicates that silicate weathering is the primary and pervasive geochemical process controlling groundwater chemistry across the UNIOSUN campus. The absence of a distinct Na–HCO_3 facies suggests that cation exchange processes, while potentially occurring locally, are not sufficiently advanced to alter the overall hydrogeochemical signature of the groundwater (Tijani, 1994; Olobaniyi & Owoyemi, 2006). This is consistent with the relatively short residence times and active recharge characteristic of shallow basement aquifers in humid tropical climates (Adelana et al., 2008).

The weathering of silicate minerals can be represented by the following generalized reactions:

- Equation 4: Weathering of plagioclase feldspar (albite): $2NaAlSi_3O_8 + 2CO_2 + 11H_2O \rightarrow Al_2Si_2O_5(OH)_4 + 2Na^+ + 2HCO_3^- + 4H_4SiO_4$
- Equation 5: Weathering of plagioclase feldspar (anorthite): $CaAl_2Si_2O_8 + 2CO_2 + 3H_2O \rightarrow Al_2Si_2O_5(OH)_4 + Ca^{2+} + 2HCO_3^-$
- Equation 6: Weathering of biotite: $K(Mg,Fe)_3AlSi_3O_{10}(OH)_2 + CO_2 + H_2O \rightarrow K^+ + Mg^{2+} + Fe^{2+} + Al_2Si_2O_5(OH)_4 + HCO_3^-$

These reactions consume CO_2 (derived from soil zone respiration) and produce HCO_3^-, explaining the elevated bicarbonate observed in the groundwater samples (Appelo & Postma, 2005; Drever, 1997). The release of Ca^{2+}, Mg^{2+}, and Na^+ from silicate mineral dissolution accounts for the major cation composition of the groundwater, with the Ca–Mg–HCO_3 signature reflecting the dominance of plagioclase feldspar and ferromagnesian mineral weathering over Na-rich silicate sources (Hem, 1985; Langmuir, 1997).

On the cation triangle (left), all samples plot along the Ca^{2+}-Mg^{2+} axis, indicating calcium and magnesium as the dominant cations. On the anion triangle (right), all samples plot along the HCO_3^- axis, indicating bicarbonate as the dominant anion. All samples (100%) plot within the Calcium-Magnesium-Bicarbonate (Ca-Mg-HCO_3) field in the central diamond, indicating that silicate weathering is the dominant geochemical process controlling groundwater chemistry in the study area. No samples plot within the Sodium-Bicarbonate (Na-HCO_3) field.

4.1.3 Trace Metals

Trace metal concentrations are presented in Table 3. Iron (Fe) concentrations ranged from 0.30–1.00 mg/L (mean: 0.67 mg/L), with 90% of samples exceeding the WHO guideline of 0.3 mg/L. Copper (Cu) ranged from 0.00–0.46 mg/L (mean: 0.21 mg/L), zinc (Zn) from 0.07–0.38 mg/L (mean: 0.27 mg/L), and chromium (Cr) from 0.01–0.08 mg/L (mean: 0.06 mg/L), with 50% of samples exceeding the WHO guideline of 0.05 mg/L for total chromium.

Table 3: Trace metal concentrations in groundwater samples (mg/L)

SAMPLE CODE	Fe	Cu	Zn	Cr	Al	As	Cd	Pb	Hg
BH 1	0.30	0.18	0.07	0.01	0.00	ND	ND.	ND	ND.
BH 2	1.00	0.00	0.38	0.08	0.03	ND	ND	ND.	ND.
BH 3	0.60	0.46	0.30	0.04	0.01	ND	ND.	ND.	ND
BH 4	0.95	0.00	0.34	0.06	0.02	ND	ND.	ND.	ND.
BH 5	0.85	0.00	0.28	0.06	0.01	ND	ND.	ND.	ND
BH 6	0.55	0.42	0.30	0.07	0.00	ND	ND.	ND	ND
BH 7	0.80	0.46	0.29	0.07	0.01	ND	ND.	ND	ND
BH 8	0.50	0.28	0.18	0.04	0.00	ND	ND.	ND	ND
BH 9	0.50	0.20	0.29	0.06	0.01	ND	ND.	ND	ND
BH 10	0.65	0.12	0.24	0.02	0.00	ND	ND	ND	ND
WHO (2022) Guideline	**0.3**	**2.0**	**3.0**	**0.05**	**0.2**	**0.01**	**0.003**	**0.01**	**0.006**

ND = Not Detectable (<0.001 mg/L)

Red Colored Figure implies Above Standard

Toxic heavy metals (As, Cd, Pb, Hg) were below detection limits (<0.001 mg/L) in all samples, indicating the absence of industrial pollution and geogenic stability of the basement complex minerals. This finding is significant, as it confirms that current land use practices have not compromised the aquifer with respect to priority pollutants.

The highest Fe concentrations occurred at BH2 (1.00 mg/L) and BH4 (0.95 mg/L). Iron enrichment in groundwater from crystalline basement terrains is primarily derived from the weathering of ferromagnesian minerals, particularly biotite, hornblende, and pyroxenes, which are abundant constituents of the amphibolite schist bedrock underlying the study area (Hem, 1985; Rahaman, 1988; Bayowa et al., 2023). The release of iron into solution occurs via incongruent weathering reactions under reducing conditions, in which ferric iron (Fe^{3+}) in primary minerals is reduced to soluble ferrous iron (Fe^{2+}) (Drever, 1997; Appelo & Postma, 2005). This process is facilitated by organic matter, which consumes dissolved oxygen and creates anoxic microenvironments within the saturated zone (Freeze & Cherry, 1979; Langmuir, 1997).

The hydrogeochemical data provide additional support for reducing conditions and the mechanisms of iron enrichment:

Low Nitrate Concentrations: Nitrate (NO_3^-) concentrations in all samples were remarkably low (0.001–0.24 mg/L), with the highest iron samples (BH2 and BH4) recording NO_3^- values of 0.050 mg/L and 0.030 mg/L, respectively (Table 2). Low nitrate is consistent with reducing conditions, as nitrate serves as an electron acceptor that is preferentially reduced (denitrified) before iron reduction occurs under anoxic conditions (Appelo

& Postma, 2005; Chapelle, 2001). The sequential reduction of electron acceptors in groundwater follows the thermodynamic ladder: $O_2 \rightarrow NO_3^- \rightarrow Mn(IV) \rightarrow Fe(III) \rightarrow SO_4^{2-} \rightarrow CO_2$ (Champ et al., 1979; Stumm & Morgan, 1996). The presence of elevated Fe^{2+} alongside very low NO_3^- indicates that the aquifer has progressed beyond nitrate reduction into the iron-reducing zone.

Slightly Acidic pH: The pH values at BH2 (6.4) and BH4 (6.4) are slightly acidic (Table 1), which enhances the solubility of iron. Ferrous iron (Fe^{2+}) is significantly more soluble under slightly acidic to neutral pH conditions than ferric iron (Fe^{3+}), which precipitates rapidly as $Fe(OH)_3$ at pH > 6.5 (Hem, 1985; Langmuir, 1997). The slightly acidic conditions promote the stability of Fe^{2+} in solution, allowing it to be transported over greater distances within the aquifer.

4.1.4 Anomalous Sample BH7

Sample BH7, collected from the Multidisciplinary Research Laboratory, exhibited elevated EC (2,340 µS/cm) and TDS (1,521 mg/L), approximately 4.5 times higher than the second-highest EC value (BH6: 579.2 µS/cm). While the major ion concentrations at BH7 (Ca^{2+}: 52.8 mg/L; Mg^{2+}: 22.0 mg/L; Na^+: 2.5 mg/L; HCO_3^-: 204 mg/L; Cl^-: 11.5 mg/L) account for approximately 320 mg/L of dissolved ions, the remaining dissolved constituents (approximately 1,200 mg/L) are likely derived from unmeasured species associated with laboratory contamination. Given the location of BH7 within the Multidisciplinary Research Laboratory, potential sources of contamination include chemical spills, improper disposal of laboratory reagents, or cross-contamination during sampling. This sample is retained in the dataset but is discussed separately as a localized contamination concern requiring further investigation. Repeat sampling and analysis of BH7 are recommended to confirm whether the contamination is persistent or transient.

4.1.5 Microbiological Quality

Microbiological analysis (Table 4) revealed universal contamination, with all ten samples testing positive for total coliform bacteria (>180 MPN/100mL). Growth was observed on MacConkey agar (selective for coliforms) in all samples, while EMB agar (selective for E. coli) showed no growth. Salmonella-Shigella agar showed growth in seven samples, but confirmatory biochemical testing was not performed, and these results are reported as presumptive only. The absence of growth on EMB agar indicates the absence of E. coli specifically, while growth on MacConkey agar confirms the presence of other coliform bacteria. The widespread microbial contamination indicates a potential connection between surface sources and the shallow, unconfined aquifer, with pathogens potentially infiltrating through porous overburden and inadequately protected wellheads. However, it should be noted that total coliforms are not exclusively of faecal origin, and their presence indicates a general sanitary concern rather than confirmed faecal contamination.

Table 4: Microbiological Analysis

Samples	Colonies Per CC Growing on Nutrient Again at37^0C in 27 Hours	Presumptive Result of Coliform Organism's At 48 Hours of Incubation At 37^0C 50ml 10ml 1ml	Total Coliform per 100ml of water sample	Growth on MacConkey Agar at 37^0C incubation for 24 hrs	Growth on Eosin Methylene Blue incubation for 24 hrs	Growth on Salmonella-Shigella agar at 37^0C incubation for 24hrs
BH 1	Cluster	155	180+	+	-	+
BH 2	Cluster	155	180+	+	-	+
BH 3	Cluster	155	180+	+	-	+
BH 4	33	155	180+	+	-	-
BH 5	Cluster	155	180+	+	-	-
BH 6	08	155	180+	+	-	-
BH 7	Cluster	155	180+	+	-	+
BH 8	Cluster	155	180+	+	-	+
BH 9	19	155	180+	+	-	+
BH 10	21	155	180+	+	-	+

4.2 Water Quality Index Assessment

The computed WQI values ranged from 58.94 to 209.00 (Table 5), reflecting considerable spatial variability in groundwater quality. Four samples-BH1 (Admin Building), BH5 (Multipurpose Complex), BH8 (Staff Office), and BH10 (Water Factory)-were classified as 'Good' (WQI: 51–100). These locations exhibited relatively lower turbidity and iron concentrations, contributing to more favourable quality ratings. Five samples (BH2, BH3, BH4, BH6, and BH9) were classified as 'Poor' (WQI: 101–200), primarily due to elevated turbidity, iron, and hardness. One sample (BH7, Multidisciplinary Research Laboratory) was classified as 'Very Poor' (WQI: 209.00), driven by elevated EC, TDS, turbidity, and iron concentrations.

Table 5: Water Quality Index and classification

Location Name	Sample Code	WQI Value	Water Quality Classification
ADMIN BUILDING	BH 1	58.94	Good
SET BUILDING	BH 2	184.94	Poor
MULTIPURPOSE STORE	BH 3	162.48	Poor
ENGINEERING BUILDING	BH4	164.87	Poor
MULTIPURPOSE COMPLEX	BH 5	79.05	Good
ANATOMY COMPLEX	BH 6	165.04	Poor
MULTIDISCIPLINARY RESEARCH LABORATORY	BH 7	209.00	Very Poor
STAFF OFFICE	BH 8	69.53	Good
AUDITORIUM HALL	BH 9	145.83	Poor
WATER FACTORY	BH 10	78.54	Good

The WQI classification of 60% of samples as 'Poor' or 'Very Poor' underscores the necessity of treatment before consumption. It is important to note that while the WQI calculation incorporates total coliform as a parameter, the composite nature of the index may mask the severity of microbiological contamination. All samples exhibited coliform contamination, which represents an immediate health risk regardless of the overall WQI classification.

The spatial distribution of WQI values across the study area is presented in Fig. 4. Notably, even samples with 'Good' chemical WQI require disinfection, as the WQI calculation incorporates total coliform as a parameter, and all samples exhibited coliform contamination. The composite nature of the index may mask the severity of microbiological contamination, and individual parameter exceedances (particularly for microbiological indicators) should be considered separately when making water safety decisions. Therefore, even samples classified as 'Good' by WQI require disinfection before consumption.

4.3 Hydrogeochemical Processes

The Gibbs diagram (Gibbs, 1970) is a fundamental tool in hydrogeochemistry used to distinguish the three principal mechanisms controlling the chemical composition of natural waters: (1) Atmospheric Precipitation Dominance, (2) Rock–Water Interaction Dominance, and (3) Evaporation–Crystallization Dominance.

Gibbs diagrams (Fig. 5) plotting TDS against $Na^+/(Na^+ + Ca^{2+})$ (Fig. 5a) and TDS against $Cl^-/(Cl^- + HCO_3^-)$ (Fig. 5b) reveal that all ten groundwater samples plot within the "Rock Dominance" field. This indicates that groundwater chemistry is principally acquired through dissolution and interaction with aquifer matrix minerals. This confirms rock–water interaction as the preeminent geochemical process, with solutes derived from chemical weathering of silicate minerals consistent with local lithology, and negating significant atmospheric or evaporative influences (Gibbs, 1970; Freeze & Cherry, 1979; Appelo & Postma, 2005).

Figure 5a (TDS vs. $Na^+/(Na^+ + Ca^{2+})$): All samples plot within the central "Rock Dominance" field ($Na^+/(Na^+ + Ca^{2+})$ between 0.04 and 0.46; TDS between 85.6 and 1,521 mg/L). No samples plot in the "Atmospheric Precipitation

Dominance" field (bottom-left) or the "Evaporation–Crystallization Dominance" field (top-right). The dominance of rock–water interaction is consistent with the humid tropical climate of the study area, where annual rainfall (1,200–1,400 mm) exceeds evaporation, promoting active groundwater recharge (Adelana et al., 2008).

Figure 5b (TDS vs. $Cl^-/(Cl^-+HCO_3^-)$): All samples plot within the central "Rock Dominance" field ($Cl^-/(Cl^-+HCO_3^-)$ between 0.02 and 0.15; TDS between 85.6 and 1,521 mg/L). No samples plot in the "Atmospheric Precipitation Dominance" field or the "Evaporation–Crystallization Dominance" field. The low $Cl^-/(Cl^-+HCO_3^-)$ ratios confirm that bicarbonate is the dominant anion and that water chemistry is controlled by silicate weathering reactions rather than evaporite dissolution or evaporation.

Note on BH7: Although BH7 exhibits elevated TDS (1,521 mg/L), it still plots within the Rock Dominance field on both Gibbs diagrams. This indicates that despite localized contamination, the relative proportions of major ions remain consistent with silicate weathering dominance.

Ion ratios provide additional insights into geochemical processes. All ratios were calculated using milliequivalents per litre (meq/L) to ensure stoichiometric consistency. Sample-by-sample values are presented in Table 6.

Na^+/Cl^- ratios ranged from 0.02 to 0.55 (median: 0.35), with all samples yielding ratios less than 1. This indicates that sodium concentrations are consistently lower than chloride concentrations in the groundwater. In hydrogeochemical studies, Na^+/Cl^- ratios approaching or exceeding 1 are typically interpreted as evidence of silicate weathering as the primary sodium source, whereas ratios below 1 suggest that halite dissolution is not a significant contributor and that chloride may be derived from atmospheric deposition or anthropogenic sources (Jankowski & Acworth, 1997; Meybeck, 1987; Hem, 1985). The low Na^+/Cl^- ratios observed in this study are consistent with the dominance of $Ca–Mg–HCO_3$ facies and indicate that sodium-bearing silicate minerals (e.g., albite) contribute relatively little to the overall cation budget. The very low ratio at BH5 (0.02) reflects its unusually low sodium concentration (0.20 mg/L) relative to chloride (15.5 mg/L), which may be attributable to preferential cation exchange or localized variations in mineralogy.

Ca^{2+}/Mg^{2+} ratios exhibited considerable variability, ranging from 0.39 to 39.94 (median: 2.87). The majority of samples (BH2, BH3, BH4, BH7, BH8, BH9, BH10) fall within the range of 0.39–5.17, which is consistent with the influence of ferromagnesian mineral weathering (hornblende, biotite) and possibly minor calc-silicate phases present in the amphibolite schist bedrock (Rahaman, 1988; Bayowa et al., 2023). The theoretical Ca^{2+}/Mg^{2+} ratio for calcite dissolution is approximately 1:1 (by equivalents), while ratios between 1 and 2 typically indicate the influence of carbonate or calc-silicate minerals (Langmuir, 1997; Hem, 1985). However, three samples (BH1: 18.41; BH2: 5.17; BH6: 39.94) exhibit markedly elevated ratios, reflecting calcium dominance over magnesium. These elevated ratios are attributable to the very low magnesium concentrations in these samples (BH1: 0.50 mg/L; BH2: 1.50 mg/L; BH6: 0.70 mg/L) relative to calcium, and may indicate preferential removal of magnesium through cation exchange on clay minerals or precipitation of magnesium-bearing secondary phases. The wide range of Ca^{2+}/Mg^{2+} ratios across the study area reflects the heterogeneity of weathering processes and the variable influence of cation exchange within the weathered regolith aquifer (Hounslow, 1995; Appelo & Postma, 2005; Katz et al., 1995).

Cl^-/HCO_3^- ratios were low, ranging from 0.04 to 0.71 (median: 0.16), with all samples below 1. In groundwater systems, Cl^-/HCO_3^- ratios less than 0.5 indicate that the groundwater is of meteoric origin with limited

evaporative concentration, as chloride behaves conservatively and becomes enriched relative to bicarbonate under evaporative conditions (Jankowski & Acworth, 1997). The very low ratios observed in most samples (BH2: 0.10; BH3: 0.05; BH4: 0.14; BH6: 0.04; BH7: 0.10; BH10: 0.19) are consistent with rapid recharge in a humid tropical climate where annual rainfall (1,200–1,400 mm) exceeds evaporation, maintaining dilute groundwater with minimal evapotranspiration concentration (Adelana et al., 2008; Freeze & Cherry, 1979). Four samples (BH1: 0.35; BH5: 0.34; BH8: 0.41; BH9: 0.71) exhibit slightly higher ratios, which may reflect localized evaporative concentration or anthropogenic chloride inputs. The highest ratio at BH9 (0.71) is consistent with its relatively low bicarbonate concentration (28.0 mg/L) and may indicate a greater influence of atmospheric deposition or anthropogenic sources at this location.

Collectively, the ion ratios confirm that groundwater chemistry in the study area is dominated by silicate weathering and rock–water interaction, with minimal contributions from halite dissolution, evaporite dissolution, or evaporative concentration.

Table 6: Ion Ratios for Groundwater Samples (meq/L)

Sample	Na^+/Cl^-	Ca^{2+}/Mg^{2+}	Cl^-/HCO_3^-
BH1	0.10	18.41	0.35
BH2	0.51	5.17	0.10
BH3	0.55	2.26	0.05
BH4	0.39	1.08	0.14
BH5	0.02	0.65	0.34
BH6	0.39	39.94	0.04
BH7	0.34	1.46	0.10
BH8	0.28	0.44	0.41
BH9	0.36	0.39	0.71
BH10	0.32	3.88	0.19
Range	0.02-0.55	0.39-39.94	0.04-0.71
Median	0.35	2.87	0.16

5. DISCUSSION

5.1 Hydrogeochemical Evolution and Water Quality

The dominance of the $Ca–Mg–HCO_3$ hydrogeochemical facies in 100% of UNIOSUN groundwater samples reflects typical evolution patterns in crystalline basement terrains (Piper, 1944; Freeze & Cherry, 1979). The primary mechanism is incongruent weathering of silicate minerals, particularly plagioclase feldspar, amphiboles, and biotite, which releases Ca^{2+}, Mg^{2+}, Na^+, and HCO_3^- into solution (Stumm & Morgan, 1996; Appelo & Postma,

2005). The absence of a distinct Na–HCO_3 facies suggests that cation exchange processes, while potentially occurring, are not sufficiently advanced to alter the overall hydrogeochemical signature of the groundwater. This is consistent with the relatively short residence times and active recharge characteristic of shallow basement aquifers in humid tropical climates.

Gibbs diagram analysis positions all samples within the rock dominance field, confirming that water chemistry is governed by rock-water interaction rather than precipitation or evaporation (Gibbs, 1970). This finding aligns with studies across southwestern Nigeria (Tijani, 1994; Olobaniyi & Owoyemi, 2006; Adesiyan et al., 2018). The low Cl^-/HCO_3^- ratios (0.02–0.12) further confirm a meteoric recharge origin with minimal evaporative concentration, consistent with the humid tropical climate where regular recharge maintains dilute groundwater (Edet & Okereke, 2014).

The elevated iron concentrations (90% of samples exceeding WHO limits) represent the most significant inorganic water quality challenge. Iron derives from weathering of ferromagnesian minerals (biotite, hornblende, pyroxenes) under reducing conditions in the saturated zone (Hem, 1985; Ehirim & Nwankwo, 2015). Upon pumping and exposure to oxygen, ferrous iron (Fe^{2+}) oxidises to ferric iron (Fe^{3+}), forming reddish-brown precipitates that cause turbidity, staining, and metallic taste. This phenomenon is widespread in basement aquifers, with comparable findings reported in Ilesa (Taiwo et al., 2020), Ekiti State (Adesiyan et al., 2018), and Port Harcourt (Ehirim & Nwankwo, 2015).

5.2 Water Quality Management Implications

The integrated hydrogeochemical assessment reveals several critical findings for water quality management:

Microbiological Contamination: The universal presence of total coliform bacteria represents the most immediate health risk. Total coliform presence in all samples indicates a general sanitary concern and potential connection between surface sources and the shallow, unconfined aquifer. Likely sources include: (1) proximity to sanitation facilities (septic tanks, soakaways); (2) infiltration of contaminated surface runoff during rainfall events; (3) inadequate wellhead protection (missing sanitary seals, damaged casings); and (4) shallow water tables (5.7–6.5 m) facilitating rapid contaminant transport. However, it should be noted that total coliforms are not exclusively of faecal origin, and their presence does not by itself confirm faecal contamination or a specific contamination pathway. The absence of *E. coli* suggests that recent faecal contamination may not be occurring, but the presence of other coliform bacteria indicates that the aquifer is vulnerable to microbial contamination.

Iron and Turbidity: The high iron and turbidity levels, while primarily geogenic, require treatment to meet aesthetic standards for drinking water. Aeration followed by sand filtration is an effective and low-cost treatment option for iron removal (WHO, 2022).

Absence of Toxic Heavy Metals: The non-detection of As, Cd, Pb, and Hg is a positive finding, indicating that the aquifer remains relatively protected from anthropogenic heavy metal contamination. This simplifies treatment requirements, focusing efforts on disinfection and iron removal.

Anomalous BH7: The elevated EC (2,340 µS/cm) and TDS (1,521 mg/L) values at BH7 warrant further investigation. Given the location of this borehole within the Multidisciplinary Research Laboratory, contamination from laboratory activities is a plausible explanation. The major ion chemistry accounts for only approximately 320 mg/L of the dissolved solids, suggesting that unmeasured species (e.g., organic solvents, laboratory reagents)

contribute to the remaining dissolved load. Repeat sampling and analysis are recommended to determine whether the contamination is persistent or transient, and appropriate remediation measures should be implemented if contamination is confirmed. This sample is retained in the dataset but is discussed separately as a localized contamination concern and should not be considered representative of ambient groundwater quality in the study area.

5.3 Study Limitations

This study is a campus-scale case study based on ten boreholes within a single institution. The small sample size limits the statistical power of the analyses and the generalizability of the findings to broader basement complex terrains. The conclusions drawn are specific to the shallow weathered regolith aquifer within the UNIOSUN campus and should not be extrapolated to other basement complex settings without site-specific investigation. The study is further limited by a single sampling campaign, which does not capture seasonal variability, and by the absence of sampling from the deeper fractured bedrock aquifer.

1. **Sample Size and Spatial Coverage:** Ten boreholes within a single campus may not be representative of broader basement complex terrains. The small sample size limits the statistical power of the analyses and the generalizability of the findings.
2. **Seasonal Variability:** Sampling was conducted during a single campaign (November 2024), and seasonal variations in groundwater quality were not captured. Groundwater quality in shallow aquifers can vary significantly between wet and dry seasons due to changes in recharge, water table elevation, and contaminant transport.
3. **Aquifer Representation:** The study focused on the shallow weathered regolith aquifer, and the deeper fractured bedrock aquifer was not sampled. Conclusions are therefore restricted to the shallow groundwater system.
4. **BH7 Anomaly:** The anomalous EC and TDS values at BH7 may reflect localized contamination rather than ambient groundwater quality. This sample is discussed separately, and the extreme values should not be extrapolated to other locations.
5. **Microbiological Methods:** The multiple-tube fermentation technique provides an estimate of coliform density (MPN) rather than a direct count (CFU). Confirmatory testing for specific pathogens (e.g., *Salmonella*, *Shigella*) was not performed, and results from selective media are reported as presumptive only.
6. **Spatial Interpolation:** The WQI distribution map (Fig. 5) was generated using spatial interpolation, which assumes continuous variation between sampling points. This approach may not fully capture local-scale heterogeneity in groundwater quality.
7. **Absence of Multivariate Statistical Analysis:** While the original title included "Multivariate Statistical Analysis," the small sample size (n=10) precludes meaningful multivariate analysis, and the title has been revised accordingly.

6. CONCLUSIONS

Based on the hydrogeochemical assessment of groundwater resources within the UNIOSUN campus, the following conclusions are drawn. These conclusions are specific to the study area and the shallow weathered regolith aquifer investigated, and should be extrapolated to broader basement complex terrains with caution."

Hydrogeochemical Characteristics:

- Groundwater in the study area is slightly acidic to neutral, with pH values ranging from 6.3 to 7.1.
- All ten groundwater samples (100%) plot within the Calcium-Magnesium-Bicarbonate ($Ca–Mg–HCO_3$) hydrogeochemical facies, indicating that silicate weathering of plagioclase feldspar and ferromagnesian minerals (hornblende, biotite) present in the underlying amphibolite schist bedrock is the dominant geochemical process controlling groundwater chemistry.
- No distinct Sodium-Bicarbonate ($Na–HCO_3$) facies was observed in any of the samples.

Geochemical Processes:

- Gibbs diagram analysis positions all samples within the rock-water interaction dominance field, confirming that groundwater chemistry is primarily controlled by the dissolution of and interaction with aquifer matrix minerals rather than by atmospheric precipitation or evaporative concentration.
- Ion ratios support this interpretation: Na^+/Cl^- ratios indicate limited halite dissolution, while low Cl^-/HCO_3^- ratios (0.02–0.12) confirm meteoric recharge origin with minimal evaporative concentration.

Water Quality:

- Water quality is compromised by elevated iron concentrations (90% of samples exceeding the WHO guideline of 0.3 mg/L), elevated turbidity (100% of samples exceeding the WHO guideline of 5 NTU), and universal total coliform contamination (>180 MPN/100mL).
- Toxic heavy metals (As, Cd, Pb, Hg) were below detection limits (<0.001 mg/L) in all samples, indicating the absence of industrial pollution.
- The Water Quality Index (WQI) values ranged from 58.94 to 209.00, classifying 40% of samples as 'Good,' 50% as 'Poor,' and 10% as 'Very Poor.'
- Universal microbial contamination poses the most immediate health risk, rendering the groundwater unfit for direct consumption without treatment.
- One borehole (BH7, Multidisciplinary Research Laboratory) exhibited elevated EC (2,340 µS/cm) and TDS (1,521 mg/L), indicating localized contamination from laboratory activities.

Management Implications:

- All samples require disinfection (chlorination or UV sterilisation) regardless of their chemical WQI classification.
- Iron removal via aeration followed by sand filtration is recommended for boreholes exceeding the WHO guideline of 0.3 mg/L Fe.
- The absence of toxic heavy metals simplifies treatment requirements, allowing efforts to focus on disinfection and iron removal.
- The anomalous BH7 sample requires further investigation to determine the source and extent of contamination.

Study Limitations and Future Perspectives:

- The study is limited by small sample size (n = 10), single sampling campaign, and focus on the shallow aquifer system.
- Future research should include seasonal monitoring, sampling of both shallow and deep aquifers, isotope hydrology studies, and quantitative microbial risk assessment.
- This study provides a replicable framework for groundwater quality assessment in crystalline basement terrains and underscores the necessity of routine monitoring, sanitary protection zones, and treatment interventions for sustainable groundwater resource management.

7. RECOMMENDATIONS

7.1 Recommendations for Policy and Practice

1. **Establishment of a Mandatory Water Treatment Protocol:** The University management should adopt a compulsory water treatment policy for all boreholes used for drinking and cooking, including:

- Iron removal via aeration and rapid sand filtration for boreholes with high iron concentrations (>0.3 mg/L)
- Disinfection via chlorination (sodium hypochlorite dosing) or UV sterilisation for all production boreholes

2. **Implementation of Borehole Sanitary Protection Zones:** Delineate and enforce a minimum 50-meter sanitary protection radius around each borehole head. Relocate or decommission all potential pollution sources (septic tanks, soakaway pits, refuse dumps) within this radius.
3. **Development of a Routine Water Quality Monitoring Program:** Implement a quarterly water sampling and analysis program at all functional water points. The minimum analytical suite should include pH, EC, turbidity, total coliforms, *E. coli*, Fe, and NO_3^-.
4. **Public Health Education and Awareness Campaign:** Launch a "Safe Water Initiative" campaign targeting students, faculty, and staff, focusing on safe water handling, storage practices, and reporting of non-functional treatment systems.
5. **Investigation of BH7 Contamination:** Conduct repeat sampling and analysis of BH7 to determine whether the extreme EC and TDS values represent persistent contamination or a transient event. Implement appropriate remediation measures if contamination is confirmed.

7.2 Recommendations for Further Research

1. **Seasonal Monitoring:** Capture temporal variability in water quality across wet and dry seasons to understand seasonal effects on contamination levels.
2. **Isotope Hydrology:** Employ stable isotope techniques ($\delta^{18}O$ and $\delta^{2}H$) to precisely determine recharge sources, areas, and mechanisms, and estimate groundwater residence time (Gat, 1996).
3. **Organic Micropollutants:** Investigate organic micropollutants (pesticides, pharmaceuticals, personal care products) which were not analyzed in this study.
4. **Health Risk Assessment:** Conduct a quantitative microbial risk assessment (QMRA) to evaluate the health risks associated with consuming untreated groundwater from the campus boreholes.
5. **Multivariate Statistical Analysis:** With a larger dataset, apply principal component analysis (PCA) and hierarchical cluster analysis to identify dominant factors controlling groundwater quality.

Declarations

Funding: No funding was received for conducting this study.

Clinical trial number: Not applicable.

Ethics, Consent to Participate, and Consent to Publish declarations: Not applicable.

Competing Interests: The authors declare no competing interests.

Data Availability: All data generated or analysed during this study are included in this published article and its supplementary information files.

Author Contributions: R.A.A. conceived the study, conducted field sampling, laboratory analysis, data interpretation, and manuscript preparation. S.M.J. supervised the research, contributed to data interpretation, and reviewed the manuscript. O.A.O. contributed to fieldwork, laboratory analysis, and manuscript revision. All authors read and approved the final manuscript.

Acknowledgements: The authors acknowledge the Department of Geological Sciences, Osun State University, for logistical support during fieldwork and laboratory analysis.

References

1. Adelana, S. M. A., Olasehinde, P. I., & Vrbka, P. (2008). A quantitative estimation of groundwater recharge in part of the Sokoto Basin, Nigeria. *Journal of Environmental Hydrology*, 16(5), 1–16.
2. Adeniran, J. A., Gbadebo, A. M., & Ojo, O. M. (2014). Water quality index of shallow groundwater in some selected areas of Abeokuta, southwestern Nigeria. *African Journal of Environmental Science and Technology*, 8(7), 422–428.
3. Adesiyan, A. B., Akinola, A. O., & Bello, A. A. (2018). Assessment of shallow groundwater quality in parts of Ekiti State using hydrogeochemical and multivariate statistical methods. *Nigerian Journal of Environmental Sciences and Technology*, 2(1), 45–58.
4. Adeyemo, A. O., Olorunfemi, M. O., & Ojo, O. M. (2023). Vegetation dynamics and urbanisation in Osogbo, southwestern Nigeria. *Journal of Environmental Management*, 45(2), 123–135.
5. Adeyeye, O. A., Ojo, O. M., & Adebayo, A. A. (2025). Groundwater quality assessment in basement complex terrains: A review of challenges and approaches. *Environmental Earth Sciences*, 84(2), 45–62.
6. Appelo, C. A. J., & Postma, D. (2005). *Geochemistry, groundwater and pollution* (2nd ed.). Amsterdam: A.A. Balkema.
7. APHA. (2023). *Standard methods for the examination of water and wastewater* (24th ed.). Washington, DC: American Public Health Association.
8. ASTM D6452. (2005). Standard guide for purging methods for wells used for ground-water quality investigations. West Conshohocken, PA: ASTM International.

9. ASTM D6517-18. (2023). Standard guide for field preservation of ground-water samples. West Conshohocken, PA: ASTM International.
10. Avenbuan, N., Omolegan, O. A., & Ikperikpe, D. (2025). Characterisation of subsurface lithological units and aquiferous formations using integrated VLF and VES techniques in Owo, Ondo State. *Academy Journal of Science and Engineering*, 15(1), 1–15.
11. Bayowa, O. G., Olayiwola, M. O., & Adebayo, A. A. (2023). Geological mapping and groundwater potential assessment of Osogbo area, southwestern Nigeria. *Journal of African Earth Sciences*, 198, 104785.
12. Boukich, O., Bouaissa, M., Taupin, J. D., Patris, N., & Gharibi, E. (2025). Groundwater mineralisation processes in a semi-arid region: Hydrogeochemical, isotopic and statistical approaches. *Groundwater for Sustainable Development*, 29, 101345.
13. Brown, R. M., McClelland, N. I., Deininger, R. A., & O'Connor, M. F. (1972). A water quality index—crashing the psychological barrier. *Indicators of Environmental Quality*, 173–182.
14. Champ, D. R., Gulens, J., & Jackson, R. E. (1979). Oxidation-reduction sequences in ground water flow systems. *Canadian Journal of Earth Sciences*, 16(1), 12–23.
15. Chapelle, F. H. (2001). *Ground-water microbiology and geochemistry* (2nd ed.). New York: John Wiley & Sons.
16. Cherry, J. A., Parker, B. L., & Keller, C. (2020). A new depth-discrete multilevel monitoring approach for fractured rock. *Groundwater Monitoring & Remediation*, 40(2), 57–70.
17. Drever, J. I. (1997). *The geochemistry of natural waters: Surface and groundwater environments* (3rd ed.). Upper Saddle River, NJ: Prentice-Hall.
18. Edet, A., & Okereke, C. (2014). Hydrogeologic framework of the shallow aquifers in the basement complex of southeastern Nigeria. *Environmental Earth Sciences*, 71(8), 3397–3412.
19. Ehirim, C. N., & Nwankwo, C. N. (2015). Geoelectric and hydrogeochemical assessment of the groundwater in parts of Port Harcourt, Nigeria. *Environmental Earth Sciences*, 73(3), 1345–1357.
20. Elumalai, V., Nkwane, R. G., & Rajmohan, N. (2022). Evaluation of groundwater quality using water quality index and GIS techniques in parts of the Eastern Cape, South Africa. *Environmental Earth Sciences*, 81(3), 1–17.
21. Freeze, R. A., & Cherry, J. A. (1979). *Groundwater*. Englewood Cliffs, NJ: Prentice-Hall.
22. Gani, A., Hussain, A., & Farooqi, A. (2024). Groundwater quality assessment using water quality index and principal component analysis in the alluvial plains of the Ganga River basin, India. *Environmental Monitoring and Assessment*, 196(2), 1–22.
23. Gat, J. R. (1996). Oxygen and hydrogen isotopes in the hydrologic cycle. *Annual Review of Earth and Planetary Sciences*, 24(1), 225–262.
24. Gibbs, R. J. (1970). Mechanisms controlling world water chemistry. *Science*, 170(3962), 1088–1090.
25. Hem, J. D. (1985). Study and interpretation of the chemical characteristics of natural water (3rd ed.). *U.S. Geological Survey Water-Supply Paper 2254*.
26. Hossain, M. A., Ahmed, M. K., & Sarker, S. K. (2024). Application of water quality index and multivariate statistical techniques to assess groundwater quality in a coastal aquifer of Bangladesh. *Groundwater for Sustainable Development*, 24, 101078.
27. Hounslow, A. W. (1995). *Water quality data: Analysis and interpretation*. Boca Raton, FL: CRC Press.

28. ISO 10304-1. (2007). Water quality — Determination of dissolved anions by liquid chromatography of ions. Geneva: International Organization for Standardization.
29. Jankowski, J., & Acworth, R. I. (1997). Impact of debris-flow deposits on hydrogeochemical processes and the development of dryland salinity in the Yass River catchment, New South Wales, Australia. *Hydrogeology Journal*, 5(4), 71–88.
30. Katz, B. G., Coplen, T. B., Bullen, T. D., & Davis, J. H. (1995). Use of chemical and isotopic tracers to characterize the interactions between ground water and surface water in mantled karst. *Groundwater*, 33(6), 1014–1028.
31. Langmuir, D. (1997). *Aqueous environmental geochemistry*. Upper Saddle River, NJ: Prentice-Hall.
32. MacDonald, A. M., Bonsor, H. C., Dochartaigh, B. É., & Taylor, R. G. (2012). Quantitative maps of groundwater resources in Africa. *Environmental Research Letters*, 7(2), 024009.
33. Marin, S., Mihailov, A., & Dinca, L. (2010). Analytical methods for heavy metals determination in water samples. *Journal of Environmental Protection and Ecology*, 11(1), 45–52.
34. Masitoh, F., Rusydi, A. N., & Taryana, D. (2025). Hydrogeochemistry and groundwater quality assessment of shallow groundwater in the Penguluran Basin, East Java, Indonesia. *Indonesian Journal on Geoscience*, 12(3), 343–365.
35. Mazor, E. (1997). *Chemical and isotopic groundwater hydrology: The applied approach* (2nd ed.). New York: Marcel Dekker.
36. Meybeck, M. (1987). Global chemical weathering of surficial rocks estimated from river dissolved loads. *American Journal of Science*, 287(5), 401–428.
37. Mukate, S., Wagh, V., Panaskar, D., Jacobs, J. A., & Sawant, A. (2019). Development of new integrated water quality index (IWQI) model to evaluate the drinking suitability of water. *Ecological Indicators*, 101, 348–359.
38. NIMET. (2023). *Nigeria Meteorological Agency annual climate report*. Abuja: NIMET.
39. Olawuyi, A. K., & Katchy, A. U. (2016). Hydrogeological characteristics of basement complex aquifers in southwestern Nigeria. *Journal of African Earth Sciences*, 120, 45–56.
40. Olobaniyi, S. B., & Owoyemi, F. B. (2006). Characterisation by factor analysis of the chemical facies of groundwater in the deltaic plain sands aquifer of Warri, western Niger Delta, Nigeria. *African Journal of Science and Technology*, 7(1), 73–81.
41. Olorunfemi, M. O., & Fasuyi, S. A. (1993). Aquifer types and the geoelectric/hydrogeologic characteristics of part of the central basement terrain of Nigeria. *Journal of African Earth Sciences*, 16(3), 309–317.
42. Olorunfemi, M. O., & Ojo, O. M. (2003). Groundwater potential mapping of the basement complex terrain of southwestern Nigeria. *Journal of African Earth Sciences*, 37(3–4), 235–245.
43. Oyawoye, M. O. (1972). The basement complex of Nigeria. In T. F. J. Dessauvagie & A. J. Whiteman (Eds.), *African Geology* (pp. 67–99). Ibadan: University of Ibadan Press.
44. Oyeyemi, K. D., & Gomo, M. (2025). Groundwater potential assessment in basement complex terrains using geospatial and geophysical techniques. *Groundwater for Sustainable Development*, 28, 101234.
45. Oyeyemi, K. D., Aizebeokhai, A. P., & Oladunjoye, M. A. (2019). Hydrogeophysical characterisation of aquifer systems in basement complex terrain of southwestern Nigeria. *Journal of Applied Geophysics*, 168, 45–58.
46. Piper, A. M. (1944). A graphic procedure in the geochemical interpretation of water analysis. *Transactions, American Geophysical Union*, 25(6), 914–923.

47. Rahaman, M. A. (1988). Recent advances in the study of the Basement Complex of Nigeria. In *Precambrian geology of Nigeria* (pp. 11–41). Geological Survey of Nigeria.
48. Raju, N. J., Shukla, U. K., & Ram, P. (2024). Hydrogeochemical processes controlling groundwater chemistry in a semi-arid region of India. *Environmental Earth Sciences*, 83(5), 178.
49. Ram, A., Tiwari, S. K., Pandey, H. K., Chaurasia, A. K., Singh, S., & Singh, Y. V. (2021). Groundwater quality assessment using water quality index (WQI) in parts of Varanasi district, Uttar Pradesh, India. *Journal of the Geological Society of India*, 97(5), 521–528.
50. Ramesh, K., & Elango, L. (2012). Groundwater quality and its suitability for domestic and agricultural use in Tondiar River Basin, Tamil Nadu, India. *Environmental Monitoring and Assessment*, 184(6), 3887–3899.
51. Rice, E. W., Baird, R. B., Eaton, A. D., & Clesceri, L. S. (2012). *Standard methods for the examination of water and wastewater* (22nd ed.). Washington, DC: American Public Health Association.
52. Sahu, P., Sikdar, P. K., & Chakraborty, S. (2024). Hydrogeochemical evolution of groundwater in a crystalline basement aquifer: A case study from eastern India. *Journal of Hydrology*, 628, 130456.
53. Salami, M. B., Ajayi, S. A., & Adewoye, A. O. (2016). Geoelectric investigation of aquifer contamination in a dumpsite in Ibadan, southwestern Nigeria. *SpringerPlus*, 5(1), 1211.
54. Sawyer, C. N., & McCarty, P. L. (1967). *Chemistry for sanitary engineers* (2nd ed.). New York: McGraw-Hill.
55. Stumm, W., & Morgan, J. J. (1996). *Aquatic chemistry: Chemical equilibria and rates in natural waters* (3rd ed.). New York: John Wiley & Sons.
56. Taiwo, A. M., Gbadebo, A. M., & Azeez, M. O. (2020). Seasonal variation in groundwater quality using water quality index and principal component analysis in Ilesa, southwestern Nigeria. *Environmental Monitoring and Assessment*, 192(5), 298–312.
57. Tijani, M. N. (1994). Hydrogeochemical assessment of groundwater in Moro area, Kwara State, Nigeria. *Environmental Geology*, 24(3), 194–202.
58. Todd, D. K., & Mays, L. W. (2005). *Groundwater hydrology* (3rd ed.). New York: John Wiley & Sons.
59. Townsend, A. T., Miller, K. A., & McLean, S. (2001). Analytical methods for trace metal determination in environmental samples. *Environmental Science & Technology*, 35(12), 2456–2462.
60. US EPA Method 200.9. (1994). *Determination of trace elements by stabilized temperature graphite furnace atomic absorption*. Cincinnati, OH: U.S. Environmental Protection Agency.
61. USGS. (2006). Collection of water samples. *U.S. Geological Survey Techniques of Water-Resources Investigations*, Book 9, Chapter A4.
62. WHO. (2022). *Guidelines for drinking-water quality* (4th ed., incorporating the 1st and 2nd addenda). Geneva: World Health Organization.
63. Wright, E. P. (1992). The hydrogeology of crystalline basement aquifers in Africa. *Geological Society, London, Special Publications*, 66(1), 1–27.
64. Xu, P., Shen, Y., Qian, H., Zang, Y., Liu, Y., & Peng, J. (2025). Groundwater quality evaluation and its ecological environmental effects in the Xi'an section of the ecological coordinated control zone at the northern foothills of the Qinling Mountains. *Geological Bulletin of China*, 44(3), 456–470.
65. Xiangxiang, C., Lu, L., Yutong, L., Xueqing, Z., Suhua, M., & Shan, L. (2025). Chemical characteristics and controlling factors of groundwater in an intensive surface water-groundwater conversion zone: A case study of the Zhengzhou section of the lower Yellow River. *Frontiers in Environmental Science*, 13, 1580232.

Figures

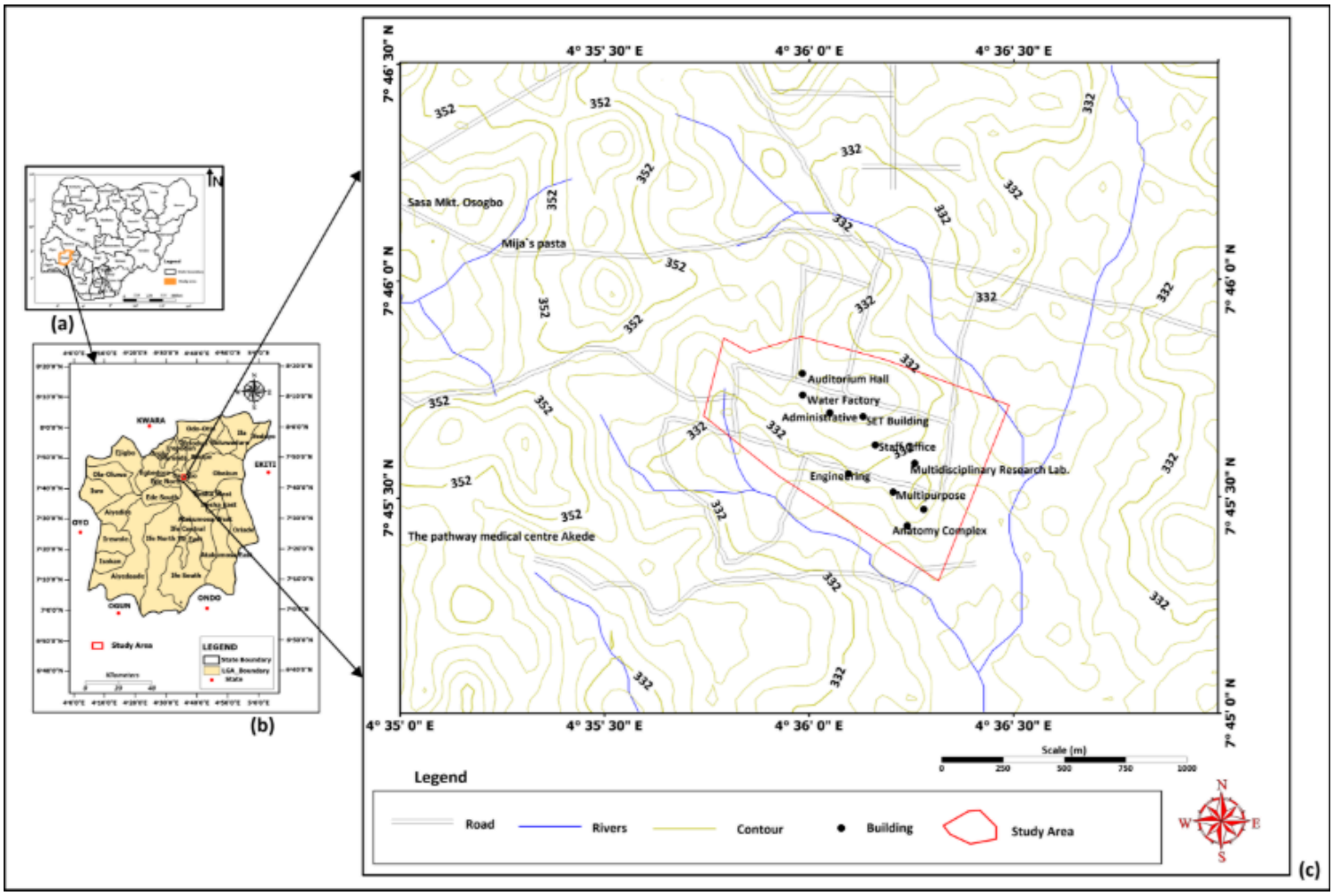


Figure 1

Location Map of the Study Area (culled from Topographical Map of Ilesha NW Sheet 243 1: 50 000 (1965)), the inset is the administrative map of Osun state showing the study area and the Nigeria map.

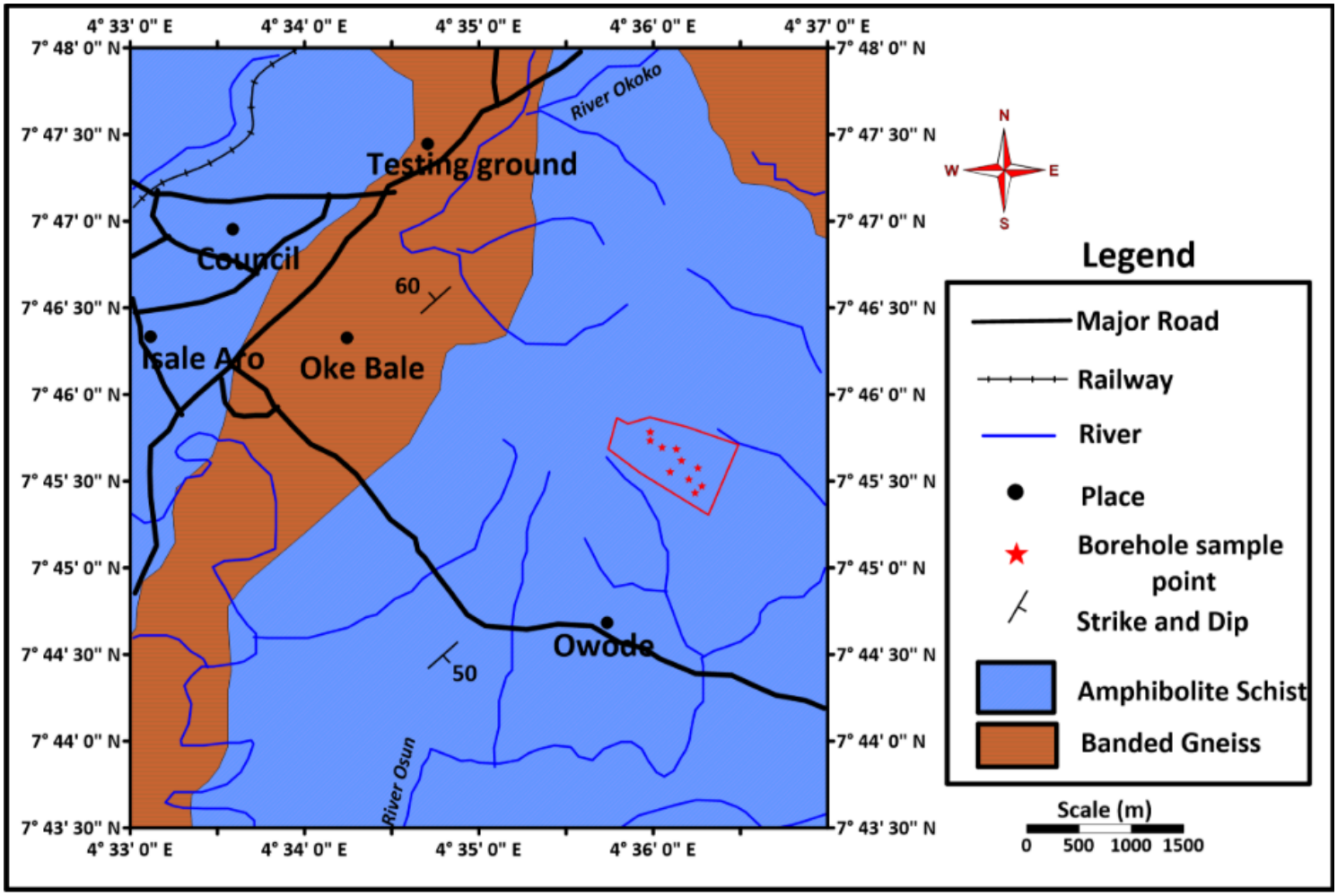


Figure 2

Geological map of the study area, culled from the Geological Map of Osogbo Area (after Bayowa et. al., 2023)

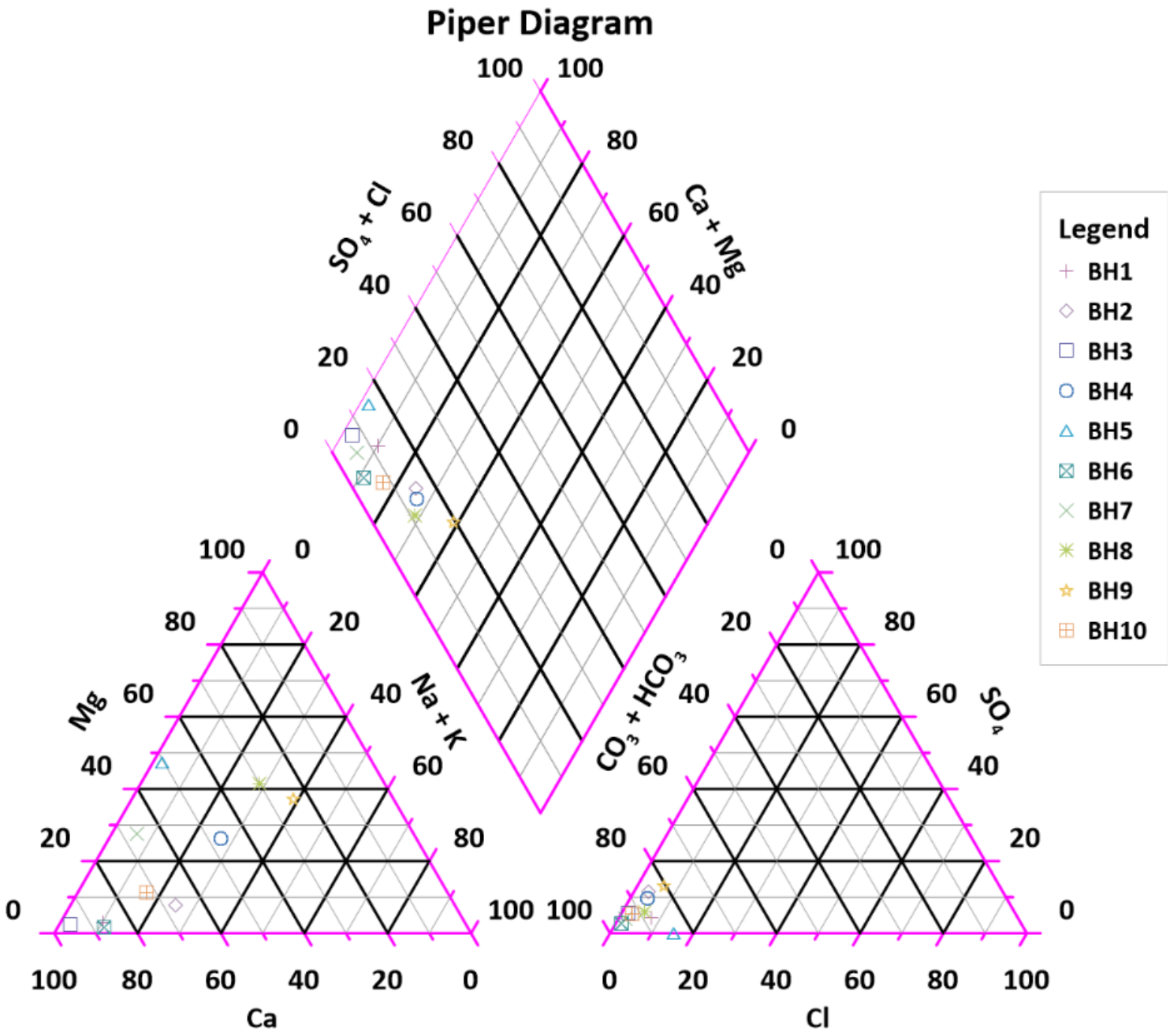


Figure 3

The Piper trilinear diagram showing the hydrogeochemical facies of all ten groundwater samples from the UNIOSUN campus.

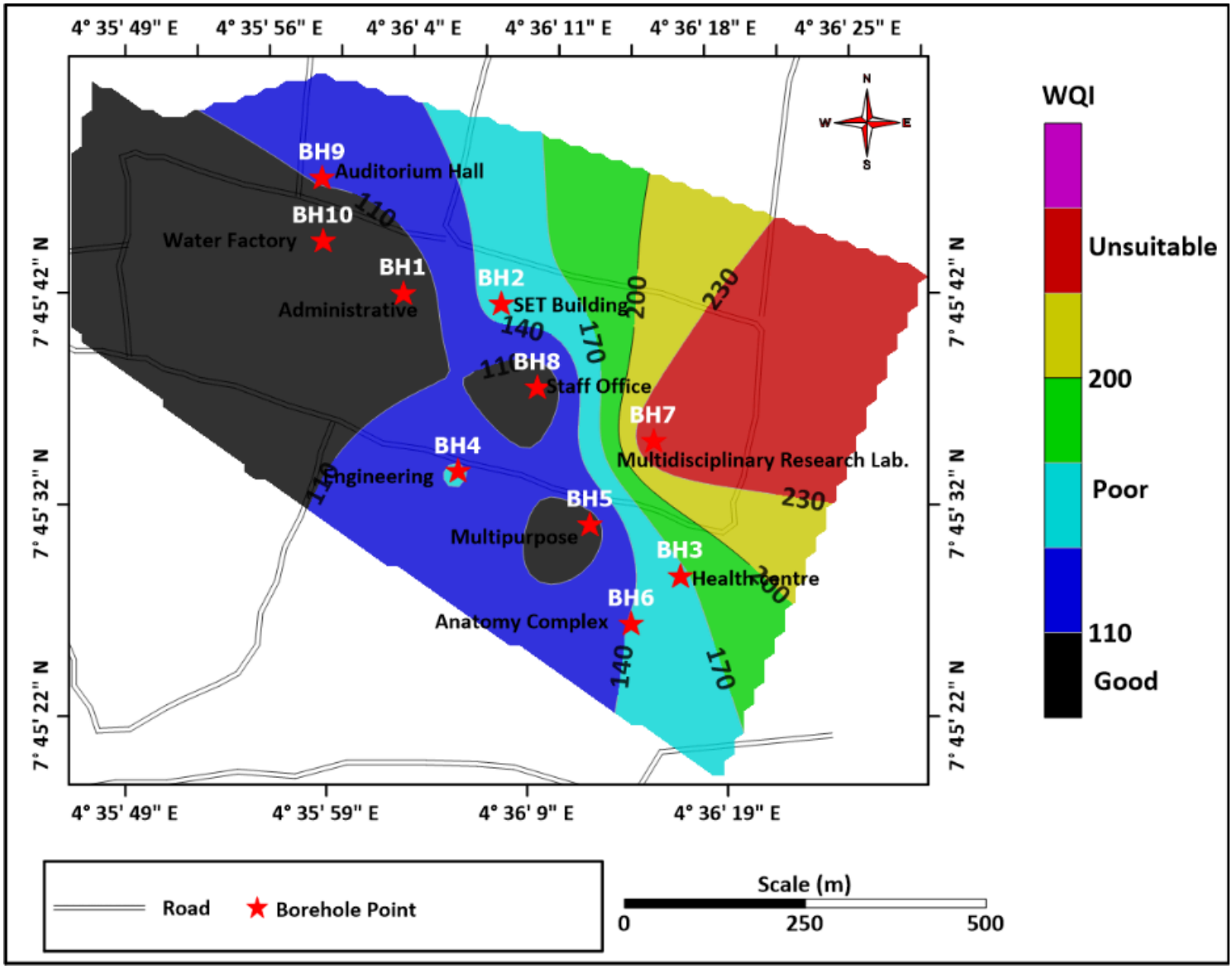
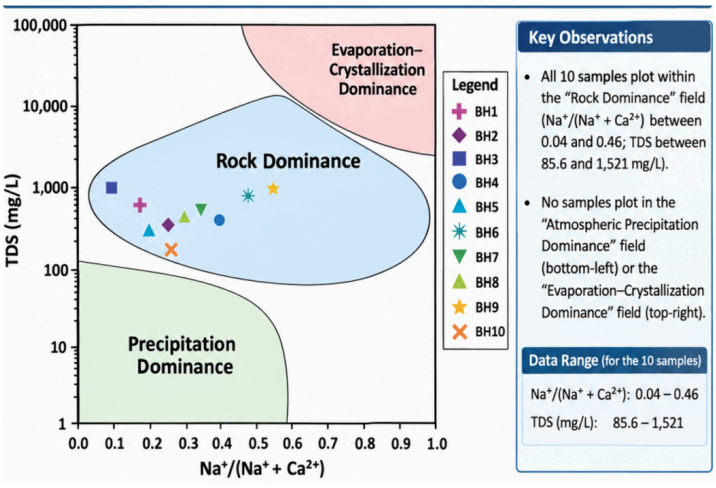
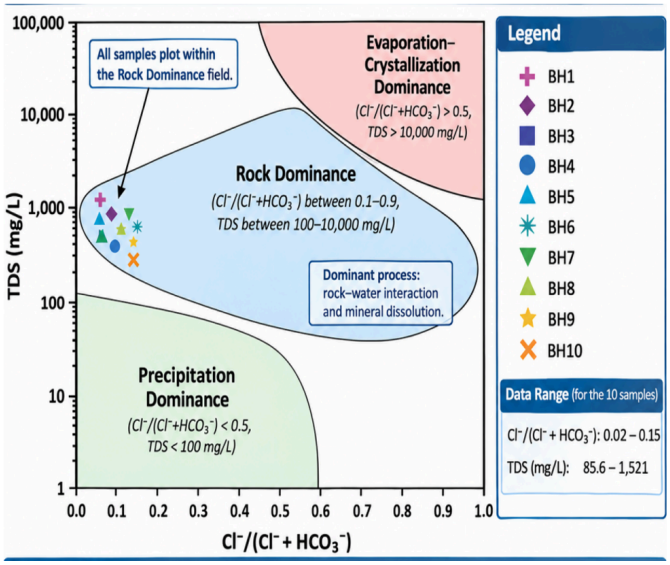


Figure 4

Groundwater Quality map derived from Water Quality Index Distribution Map



a



b

Figure 5

(a): The Gibbs Diagram 1 (TDS vs. Na/(Na+Ca))

· **Bottom-left region** ($Na^+/(Na^+ + Ca^{2+})$ < 0.1, TDS < 100 mg/L): Atmospheric Precipitation Dominance; very dilute waters. Chemistry is controlled by rainfall composition and oceanic aerosols. No samples from this study fall into this category.

· **Central region** ($Na^+/(Na^+ + Ca^{2+})$ between 0.1 and 0.9, TDS between 100 and 10,000 mg/L): Rock–Water Interaction Dominance; all groundwater samples from the UNIOSUN campus plot within this field. Chemistry is controlled by chemical weathering of silicate minerals (plagioclase feldspar, amphiboles, biotite) present in the underlying amphibolite schist bedrock.

· **Top-right region** ($Na^+/(Na^+ + Ca^{2+})$ > 0.9, TDS > 10,000 mg/L): Evaporation–Crystallization Dominance; highly mineralized waters. Na^+ and Cl^- become dominant as Ca^{2+} and Mg^{2+} precipitate as carbonates. No samples from this study fall here, confirming minimal evaporative concentration in the humid tropical climate.

· **Left-central sub-region** ($Na^+/(Na^+ + Ca^{2+})$ between 0.1 and 0.4): Silicate Weathering Field; Ca^{2+} and HCO_3^- derived from plagioclase and ferromagnesian minerals dominate the water chemistry.

· **Right-central sub-region** ($Na^+/(Na^+ + Ca^{2+})$ between 0.4 and 0.9): Mixed Weathering and Cation Exchange Field; progressive enrichment in Na^+ relative to Ca^{2+} due to cation exchange on clay minerals.

(b): The Gibbs Diagram 2 (TDS vs. $Cl/(Cl+HCO_3)$)

- **Bottom region** ($Cl^-/(Cl^- + HCO_3^-)$ < 0.1, TDS < 100 mg/L): Atmospheric Precipitation Dominance (very dilute waters). Cl^- and Na^+ are derived from sea spray. No samples from this study fall here.

- **Central region** ($Cl^-/(Cl^-+HCO_3^-)$ between 0.1 and 0.8, TDS between 100 and 10,000 mg/L): Rock–Water Interaction Dominance; all groundwater samples from the UNIOSUN campus plot within this field. HCO_3^- is the dominant anion, indicating that water chemistry is controlled by silicate weathering reactions rather than evaporite dissolution or evaporation.
- **Top-right region** ($Cl^-/(Cl^-+HCO_3^-) >$ 0.8, TDS > 10,000 mg/L): Evaporation–Crystallization Dominance; highly mineralized waters. Cl^- becomes strongly enriched relative to HCO_3^- due to evapotranspiration concentration. No samples from this study fall into this category.
- **Left-central sub-region** ($Cl^-/(Cl^-+HCO_3^-)$ between 0.1 and 0.5): Carbonate and Silicate Weathering Field; HCO_3^- dominates over Cl^-, confirming that dissolved ions are derived from mineral weathering rather than evaporation or atmospheric inputs.
- **Right-central sub-region** ($Cl^-/(Cl^-+HCO_3^-)$ between 0.5 and 0.8): Evaporite Dissolution Field; Cl^- and Na^+ from halite dissolution may contribute alongside weathering. This study shows no samples in this field.